JOURNAL OF GEOPHYSICAL RESEARCH, VOL. 100, NO. B3, PAGES 3859–3871, MARCH 10, 1995

Simulation of magnetic hysteresis in pseudo-single-domain grains of magnetite

W. Williams

Department of Geology and Geophysics, University of Edinburgh, Edinburgh, Scotland

David J. Dunlop

Department of Physics, University of Toronto, Toronto, Ontario, Canada

Abstract. Magnetic hysteresis has been simulated in grains of magnetite for the size range 0.1-0.7 μm. This was achieved using an unconstrained three-dimensional micromagnetic model of single grains of magnetite with cubic magnetocrystalline anisotropy. Hysteresis loops were obtained for fields applied along both the easy and hard magnetocrystalline axes. Both discrete (Barkhausen) jumps and gradual changes in the magnetic structure are seen, and the reversal of the magnetization can be followed from near saturation in a normal field to a similar state in a reverse field. Predictions of coercivity agree well with published experimental data for unstressed cubic grains of magnetite.

Introduction

Magnetic hysteresis is used as a primary indicator of magnetic mineralogy and domain state in samples used in rock and mineral magnetism. Hysteresis loops give an indication not only of mineral type but also of the grain size through the observed mechanism of reversal of the magnetization. Domain switching during hysteresis is usually described in terms of coherent rotation of magnetization in single-domain (SD) grains or as movement of well-defined domain walls in multidomain (MD) grains. However, the switching mechanisms for grains of intermediate sizes (i.e., pseudo-single-domain (PSD) grains) are poorly understood. These processes are best modeled using three-dimensional micromagnetic simulations which are able to model the inhomogeneous magnetizations that are likely to exist. The validity of these models can presently only be verified by comparison with experimental measurements in bulk samples of PSD grains, since direct observations of domain structures in submicron grains are not yet possible.

Three-Dimensional Models of Magnetic Structures

The micromagnetic models used to obtain the magnetic structures at each point in the hysteresis loops have been described elsewhere [*Williams and Dunlop*, 1989, 1990; *Schabes and Bertram*, 1988a]. A magnetic grain is subdivided into a three-dimensional grid of cubic cells in which a single vector at the center of a cell is used to represent the average direction of the magnetization of that cell. Each magnetic structure represents a minimum energy state, although not necessarily an absolute energy minimum. The magnetic energy is composed of four parts: the self-demagnetizing energy, the exchange energy, the magnetocrystalline anisotropy energy, and the external field energy. The most notable exclusion is the magnetoelastic energy (this is a complicated and computationally expensive energy to calculate), whose contribution is at least an order of magnitude smaller than the other contributions to the total free energy in magnetite.

The grains are assumed to be perfect parallelepipeds (cubes) unless otherwise stated. All solutions shown represent structures at 25°C, and the magnetocrystalline anisotropy easy axes are along the <111> directions, where <100> are the grain edges.

Simulation of Hysteresis

We attempted to model as closely as possible the experimental procedure for obtaining hysteresis loops in real samples of magnetite. The initial magnetic state was a remanence structure after saturation. It was not possible to start from an alternating field demagnetized state since this would have required large amounts of computer time to simulate. In any case, the magnetic structures of the grains determined during hysteresis were not sensitive to the initial magnetic structure. The field is then applied along a particular direction and increased to 150 mT in steps of 10 mT. A complete hysteresis loop is performed where the field is reduced to −150 mT and increased back to +150 mT in 2-mT steps. The initial guess for minimization of the energy

Paper number 94JB02878.
0148-0227/95/94JB-02878$05.00

at each field step was taken as the final solution of the minimization from the previous field step. The peak field values of the hysteresis loops were chosen to be the same as those used in hysteresis experiments by *Dunlop* [1986] on PSD-sized grains of magnetite. In some cases this meant that saturation of the magnetization was never achieved during hysteresis. The magnetization intensity of the grain was calculated as that component lying along the direction of the external field.

Successive solutions at small differences in applied magnetic field represent closely related local energy minimum (LEM) magnetic structures. As the field strength changes, the magnetic structure will follow a minimum energy path to the next metastable state. The hysteresis loop is therefore represented by a series of metastable states and not true dynamic states [see *Schabes*, 1991]. Thus in the *Landau and Lifshitz* [1935] equation

$$\frac{d\mathbf{M}}{dt} = \gamma_0\mu_0\mathbf{M} \times \mathbf{H}_{eff} - \frac{\lambda}{\mathbf{M}_s^2}\mathbf{M} \times (\mathbf{M} \times \mathbf{H}_{eff})$$

we assume infinite damping so that the second term on the right hand side is set to zero, and $d\mathbf{M}/dt = 0$ since we are considering a series of quasi-static states, appropriate to the simulation of experimental measurement of hysteresis loops. The remaining term is the torque acting on the magnetization and must be zero for stable or metastable states; that is, $\mathbf{M}$ should be parallel to $\mathbf{H}_{eff}$. $\mathbf{H}_{eff}$ is an effective field acting on the magnetization due to the demagnetizing, exchange and magnetocrystalline anisotropy energies.

We have neglected the effects of thermal fluctuations, because the energy barriers in the grain sizes being considered are much larger than 25 kT (where k is the Boltzman constant, and T here is the temperature). As an example, consider the 0.05 μm and 1.0 μm grains, which, from the models described in this paper, have predicted coercivities of about 20 mT and 3 mT, respectively. As a zeroth-order approximation we may consider the energy barrier to reversal of the magnetization as simply that for coherent rotation of the magnetization, and so $\Delta E = \frac{1}{2}\mu_0 H_c M_s V$, where H_c is the coercivity, M_s is the saturation magnetization, and V is the grain volume. This yields energy barriers of 1.32×10^{-18} J and 1.44×10^{-15} J for the 0.05 μm and 1.0 μm grains respectively, compared to a 25°C value of 25 kT of 1.1×10^{-19} J. The barriers to changes in the directions of magnetization are therefore several orders of magnitude larger than the energy provided by thermal fluctuations.

Coherent Rotation in Single-Domain Grains

Before discussing the results of the numerical models it is worth considering the theory of coercivity for single-domain grains. For magnetite, the anisotropy energy is given by

$$E_K = K_1(\alpha_1^2\alpha_2^2 + \alpha_2^2\alpha_3^2 + \alpha_3^2\alpha_1^2)V$$

where $K_1 = -1.35 \times 10^4$ J m^{-3} is the anisotropy constant and the α are the direction cosines of the magnetizations. The second order anisotropy term K_2 has been neglected.

The energy barrier to coherent rotation can be easily determined when the path that the magnetization takes during rotation is known. The maximum resistance to reversal will occur when the magnetization rotates though a hard <1 1 1> direction, and the resulting coercivity of the grain is calculated [e.g., *Stacey and Banerjee*, 1974] as

$$\mu_0 H_c = \frac{4}{3}\frac{K_1}{M_s}.$$

For such coherent rotation of magnetization, the energy surface of the grain can be mapped out as the external magnetic field applied to the grain is changed. Figure 1 shows the three-dimensional energy surface for a cubic grain of magnetite at 25°C. The easy and hard axes are easily identified by the minima and maxima in the energy surface, respectively. As the external field along $[\bar{1}\ \bar{1}\ \bar{1}]$ changes, the energy surface deforms, and at a field equal to H_c the local energy minimum around the easy axis disappears and allows the magnetization to rotate along the minimum energy path toward the external field direction. For magnetite at room temperature, K_1 and M_s take the values -1.35×10^4 J m^{-3} [*Flecher and O'Reilly*, 1974] and 4.8×10^5 A m^{-1} [*Heider and Williams*, 1988], respectively, giving a coercivity of $\mu_0 H_c \approx 37.5$ mT. This should be the maximum possible coercivity for cubic grains, since coherent rotation of the magnetization should be a possible magnetization reversal mode for any domain state configuration. Significantly reduced coercivities should result for noncoherent rotation, which may occur in uniform as well as nonuniform domain states.

It is expected that the coercivity of the grain will depend upon the direction of the external field with respect to the grains' easy axes of magnetization. This is certainly true for small grains that undergo coherent rotation. The predicted hysteresis loop for a random assembly of such grains is determined by integrating the orientation-dependent hysteresis values over a hemisphere [*Stoner and Wohlfarth*, 1948]. In the case of grains where coherent rotation of the magnetization does not occur, we must investigate the magnetic switching mechanism as a function of grain orientation with respect to the applied field. Since the simulation of magnetic structures during hysteresis is a computationally expensive calculation, we examined only the coercivities for fields applied along the easy and hard axes.

Results

Magnetic structures during hysteresis for PSD grains of magnetite of sizes 0.1 μm to 1.0 μm are described below. Figures 2-6 show the hysteresis loops for fields

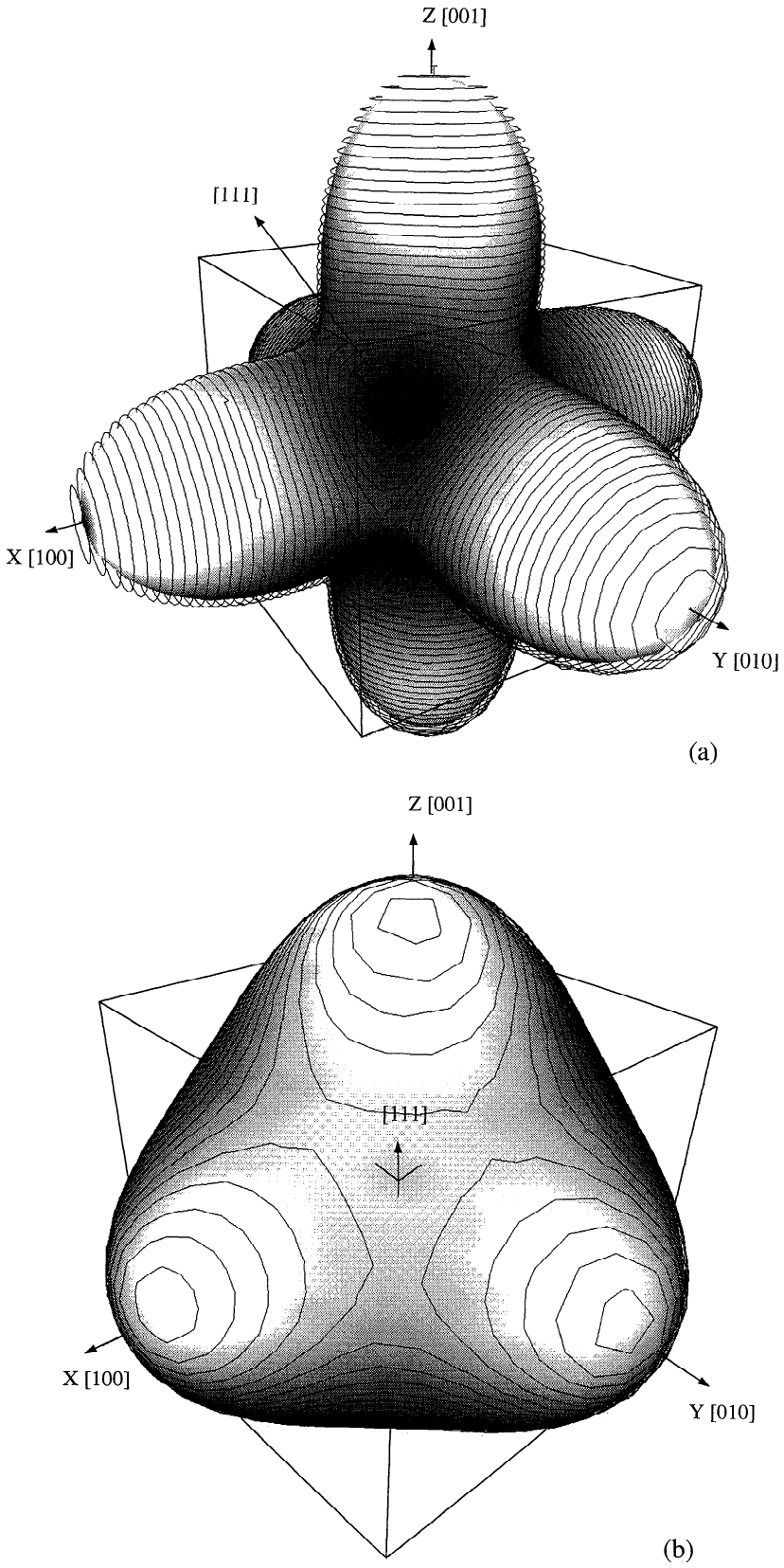

Figure 1. The three dimensional energy surface of a cubic grain of magnetite with cubic anisotropy. The shaded regions represent low energy and the light high energy. (a) The zero applied field state. Here the hard magnetocrystalline axes can be seen as the high-energy regions and correspond to the three <100> crystalline axes. (b) The deformed energy surface as a magnetic field is applied along an easy axis directly into the page. The energy of the easy direction facing out of the page now increases. When the external field strength equals the coercive force value, there will be no minimum energy state in this direction.

applied along the magnetocrystalline hard axis, Figure 7 for fields applied along the easy axis, and Figure 8 for elongated grains.

The initial zero-field states (before hysteresis cycling) are saturation remanence states, where the field was sufficient to perfectly align the magnetization. In the models where the field was applied along a hard <001> axis, the zero-field magnetic structures do not relax toward a magnetocrystalline easy <111> axis, suggesting that in these size grains the magnetocrystalline anisotropy is not very influential.

The grain is then taken through a hysteresis loop which first increases the field from 0 to +150 mT in 10-mT steps and then completes a loop in 2-mT steps from +150 mT to −150 mT and back to +150 mT. The final magnetic structures obtained at the end of the ascending branch of the hysteresis loop were in all cases identical to the structures obtained at the start of the descending branch (with the exception of the 0.1-μm grain), so that further cycling of the field, with the same peak field value, would have produced identical hysteresis loops.

Solutions for Fields Applied Along Hard Axis

Results for a 0.1-μm grain. The initial zero field stable state for this structure is the flower [*Schabes and Bertram*, 1988a] or 1Λ state [*Williams and Dunlop*, 1989], which is simply the single-domain state (with a remanence of 92% of that of saturation) with deformation of the magnetization from the uniform state near the grain surface (see Figure 2b). This state persists as the field is increased to between 40 and 50 mT (see Figure 2a), when the magnetization flips instantaneously to a flower state in the opposite direction.

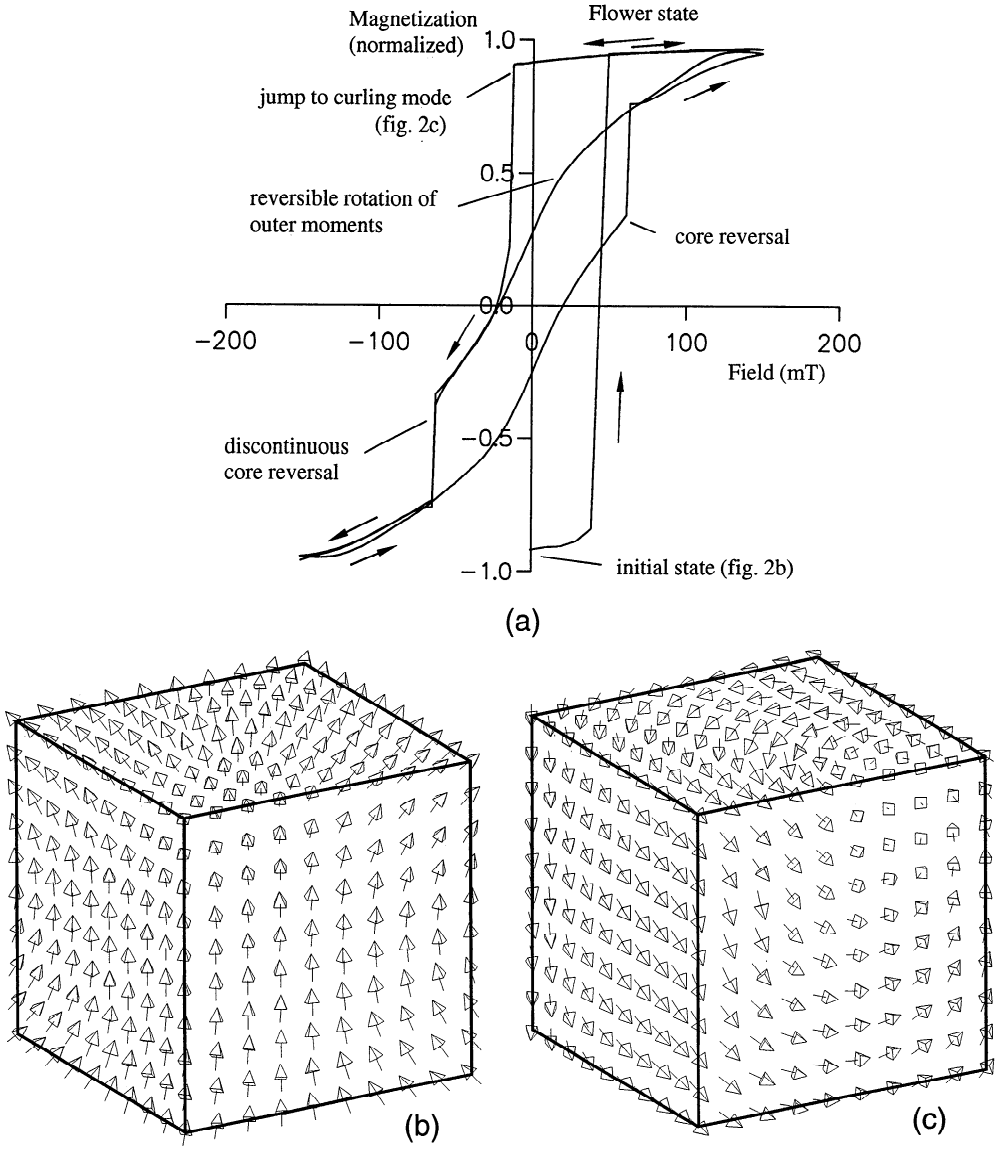

Figure 2. (a) The hysteresis loop for a 0.1-μm cube of magnetite for the field directed along the [001] hard axis. (b) The initial zero-field magnetization state of the grain after complete saturation along the [001] axis (-z direction). (c) The curling or vortex mode achieved on reduction of the field to −14 mT in the second and subsequent hysteresis cycles.

This flower state is not the lowest energy state available to this grain, however, and on cycling to negative fields, the magnetization jumps to a curling mode structure (Figure 2c). This type of magnetic structure was not obtained in a previous study [*Williams and Dunlop*, 1990] since only true saturation remanence structures (i.e., from a true saturating field) were modeled. Curling mode structures have been reported, however, for example, by *Schabes and Bertram* [1988a], who referred to such magnetizations as vortex structures.

This curling mode state persists for all further hysteresis cycles. The magnetization reverses the direction of the domain's magnetization by gradual rotation of the outer layers of magnetization, leaving a cylindrical core domain magnetized in opposition to the external field. At a reverse field of 64 mT the core domain switches in a single Barkhausen jump to align with the external field.

Results for a 0.2-μm grain. As the grain size is increased, a flower state cannot be accommodated because of the increased internal demagnetizing energy. The initial state is similar to a 1B type solution (Figure 3b) [see *Williams and Dunlop*, 1989] where the magne-

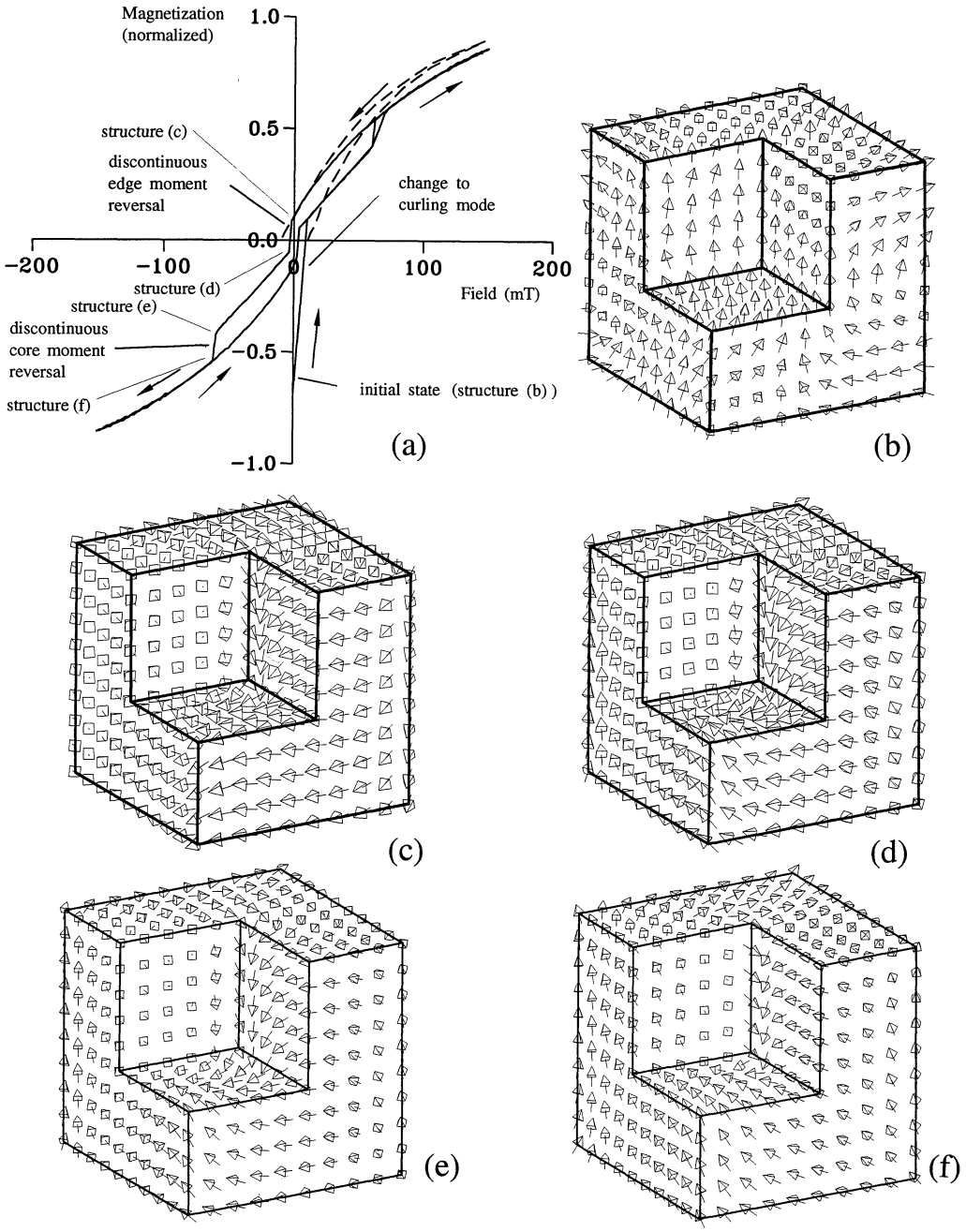

Figure 3. (a) The hysteresis loop for a 0.2-μm cubic grain of magnetite; field along the hard axis. The dashed line shows the experimental data for a sample containing magnetite grains with a mean size of 0.22 μm [*Dunlop*, 1986] (b) The initial domain state in zero field is a 1B-type solution [see *Williams and Dunlop*, 1989]. The magnetization undergoes two Barkhausen jumps: first, the grain's edges reverse, as shown (c) before and (d) after the jump, and then the core domain reverses via a Barkhausen jump shown (e) before and (f) after the jump.

tization at the grain edges forms domain structures distinct from the near-uniform magnetization of the grain center. However, this is a weak LEM state, since it changes to a curling mode immediately when the minimum reverse field step is applied.

The larger grain is now capable of maintaining a more complex domain structure, and thus we may expect more complex states during reversal of the magnetization. We now obtain two Barkhausen jumps in each half of the hysteresis cycle. As the external magnetic field is reduced from zero, the first Barkhausen jump occurs as the magnetization at the vertical edges reverses (see Figures 3c and 3d). The volume of the edge domains then increases by moving the transition region between the outer moments and the core (i.e., the domain wall) toward the core of the grain, then as the reverse field is increased further, the core domain reverses (Figures 3e and 3f) and produces a Barkhausen jump at about the same field intensity as that of the core reversal in the 0.1-μm grain.

Because a Barkhausen jump large enough to reverse the net magnetization occurs at a small field of -2 mT, the coercivity appears to be well defined and takes a value of 3.2 mT. This is unusually low for this grain size range. However, experimentally, we would not expect to be able to distinguish the Barkhausen jumps in assemblies of real grains, in which both the grain size and field orientation vary.

Results for a 0.3-μm grain. As with the 0.2-μm grain the initial state is 1B, and this quickly transforms to the curling mode upon application of a small field (see Figure 4a). The zero-field stable state is similar to that shown for the 0.2-μm grain (Figure 3d) and has a reversely magnetized core domain and four normally magnetized domains at the grain edges, so that on application of a reverse field, the core domain grows out toward the grain edges until at a field of -42 mT the edge domains reverse via a Barkhausen jump. After both the grain core and edges have aligned with the ex-

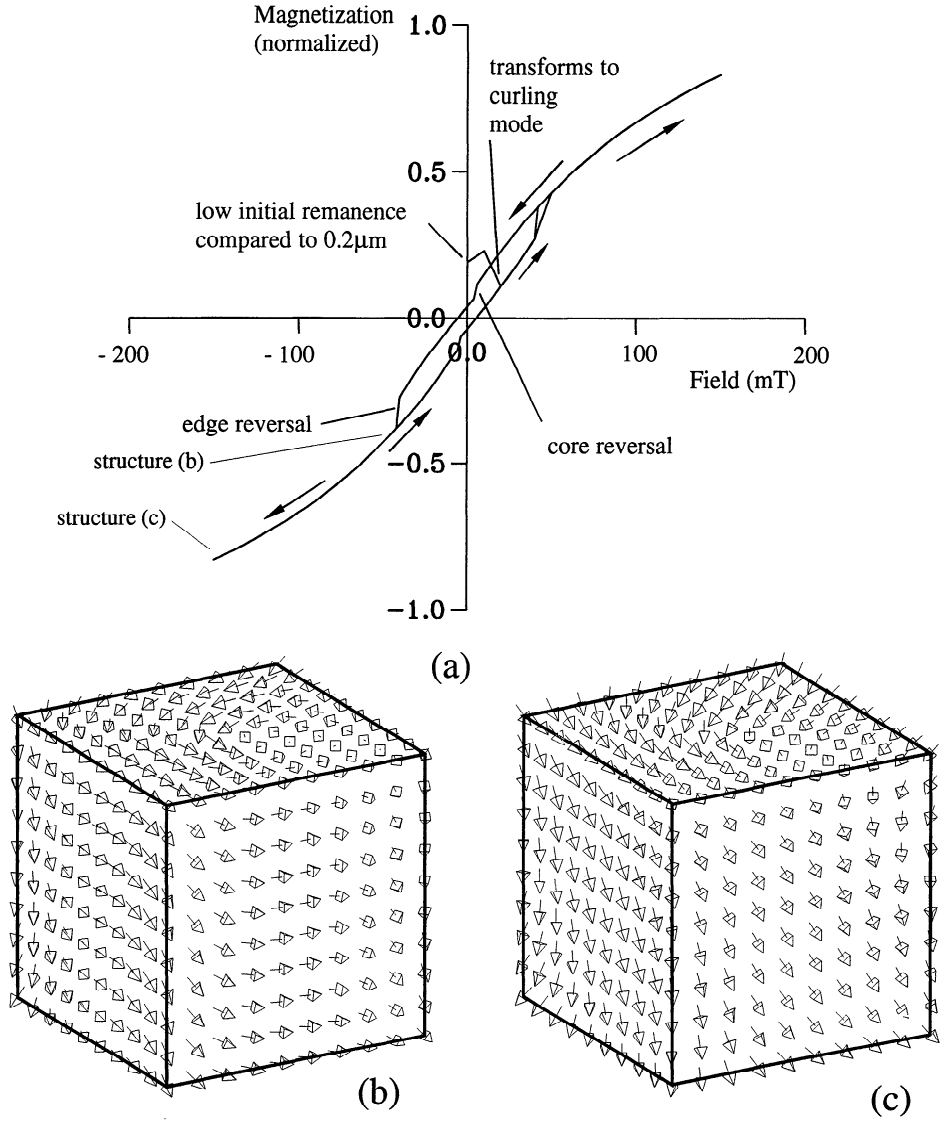

Figure 4. (a) The hysteresis loop for a 0.3-μm cubic grain of magnetite; field along the hard axis. The magnetic structure at (b) -42 mT and (c) at -150 mT, showing the gradual rotation of the magnetization towards the external field direction, after the Barkhausen jumps of the core and edge domains.

ternal field, the magnetization near the centers of the grain faces gradually rotates toward the field direction as the grain magnetization approaches saturation (Figures 4b and 4c).

Results for a 0.5-μm grain. The initial stable state is now a curling mode but with the core and edge magnetizations in opposite directions (similar to Figure 3d). As the field is reduced from 150 mT along the descending loop, the core reverses at a field of 36 mT (compare 6 mT for the 0.3-μm grain). The edge domains do not start to reverse until the field is reduced past zero. They do not reverse via a single Barkhausen jump but via several smaller discrete jumps at -34 mT, -70 mT, and -92 mT (Figure 5) as the core domain grows out toward the grain edges.

Results for a 0.7-μm grain. The zero-field initial state is now much more complex. It is no longer a simple curling or vortex state, but is characterized by a more lamellar structure forced by the increasing influence of the magnetocrystalline anisotropy energy, which tends to rotate the magnetization out of the horizontal toward the easy <111> directions. Three more or less antiparallel domains can be seen on the grain surface (Figure 6b). However, we have not yet achieved a true lamellar state as seen in Bitter pattern experiments on larger grains of magnetite, and the 0.7-μm grain solution is still significantly influenced by the vortex structures seen in the smaller grains.

As the field is reduced from saturation, the core domain first reverses (in a series of jumps), then as the field increases in the opposite polarity, the central domain, which is now aligned with the field, increases in size. The central domain is defined roughly by the domain wall shaded in Figure 6c. As the field is increased toward a maximum of +150 mT, there is a gradual movement of this domain wall, indicated by the domain wall at the grain surface moving toward the left in Figures 6d-6f. This is the first three-dimensional micromagnetic simulation of smooth domain wall movement under the influence of external fields. It should be noted that the domain wall here is not of classical Bloch or Néel type since its form varies as it approaches the grain surface. However, at the grain center the rotation of the magnetization within the wall is normal to the plane of the wall (Figure 6c) and so can be said to show Néel characteristics. The 0.7-μm grain thus marks the boundary between the smaller grains where magnetization reversal occurs via Barkhausen jumps and the larger grains dominated by domain wall motion.

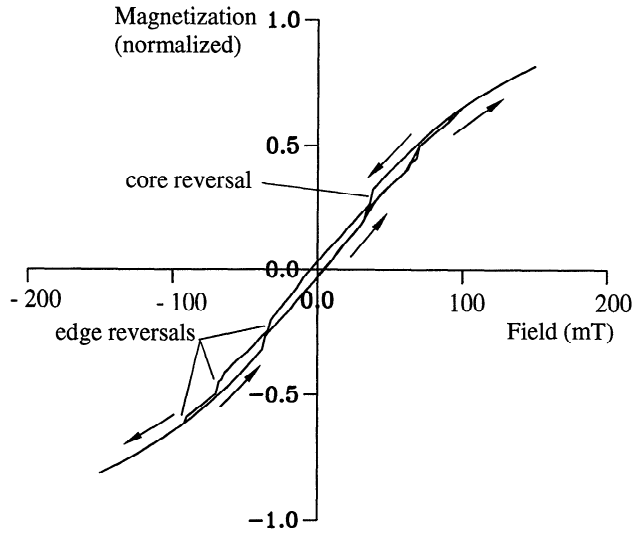

Figure 5. The hysteresis loop for a 0.5-μm cubic grain of magnetite; field along the hard axis.

Solutions for Field Applied Along Easy <111> Axis

Similar calculations with the field applied along a <111> easy axis were carried out for 0.1-μm, 0.2-μm, 0.5-μm, 0.7-μm, and 1.0-μm size grains. The resulting hysteresis loops are shown in Figure 7a. Since the magnetization prefers to lie along an easy axis, the magnetization intensity at peak fields is always greater than that observed for hysteresis along the hard direction.

In the smallest grain size (0.1-μm), the stable zero-field state is the flower state aligned along the [111] axis (Figure 7b), and the magnetization reversal occurs via a vortex state. During reversal of the magnetization of the grain, the vortex state is found to be stable in fields of between 24 mT and 72 mT; otherwise, the flower state is the only stable domain configuration. In larger grains, essentially the same process occurs: the structure transforms from a flower state aligned with the [111] easy axis to similar antiparallel structure via a vortex state. For grains of sizes 0.2 μm and larger, the switching process is gradual, and the mechanism can be seen to be vortex propagation, where a vortex structure is nucleated at one end of the grain and propagates to the other end, reversing the magnetization, as shown in Figures 7c-7e (see also *Enkin and Williams* [1994]).

In general, there are fewer Barkhausen jumps when the field is applied along the easy direction. As a consequence, the anomalously low saturation remanence exhibited by the 0.2-μm grain for hysteresis along the hard direction is now not observed.

Solutions for an Elongated Grain

The effect of grain elongation was examined for a particular grain size of $0.3 \times 0.3 \times 0.5$ μm, and for the cases where the external field was applied along (1) its short axis, (2) its long axis, and (3) the easy magnetocrystalline [111] axis. The corresponding hysteresis loops are shown in Figure 8a.

In each case the zero-field domain configuration is a vortex state which has its vortex axis aligned with the direction of the external magnetic field (see Figure 8b). In all three cases, the mode of domain reversal was by vortex propagation, as described in the section above. Grain shape has much less effect on coercivity and saturation remanence than it would have if the magnetization had reversed by coherent rotation. The coercivities and saturation remanences of these grains

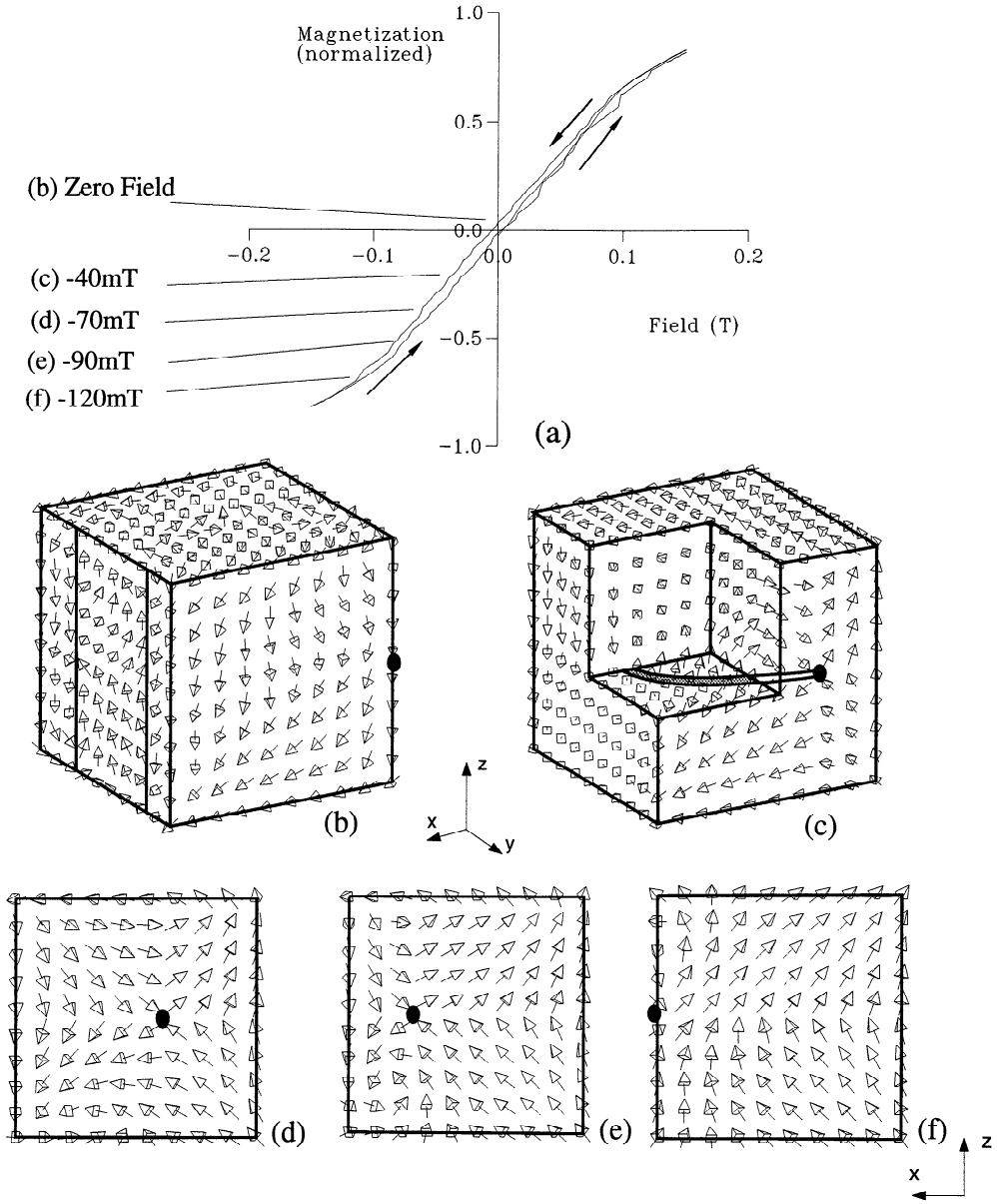

Figure 6. (a) The hysteresis loop for a 0.7-μm cubic grain of magnetite; field along the hard axis. (b) The initial zero-field magnetic structure, exhibiting lamellarlike features on the grain faces, with the magnetization lying parallel to the grain surface and in a plane containing an easy magnetocrystalline axis. Smooth movement of domain walls occurs as the core domain gradually grows out from the center. (c) The cutaway view of the grain in a 40 mT field shows the domain wall (shaded area) separating the surface and core domains. The gradual rotation of the surface magnetization is shown in fields of (d) 70 mT, (e) 90 mT, and (f) 120 mT.

are about the same as those of cubic grains of similar sizes containing vortex states, although case (3) yields slightly lower values.

Discussion

The general features of the results can be explained as follows. In the smaller grains (0.1 μm, 0.2 μm), the vortex mode, with both the core and surface magnetization pointing toward the $+z$ [001] direction, is a stable state at zero field. The magnetic structure of these smaller grains is controlled by exchange coupling rather than demagnetizing energy, and so as a reverse field is applied, the outer layer of the grains' magnetization rotates first, since the exchange coupling of the outer layer is not as strong as that of the interior magnetization, because of the proximity of the free surface of the grain. The exchange coupling in the 0.1-μm grain is strong enough to ensure a continuous rotation of the surface magnetization, while in the 0.2-μm grain the magnetization of the four grain edges in the z direction rotates by a Barkhausen jump.

In larger grains (i.e., above $\sim$ 0.3 μm) the demagnetizing fields begin to dominate, and, although the vor-

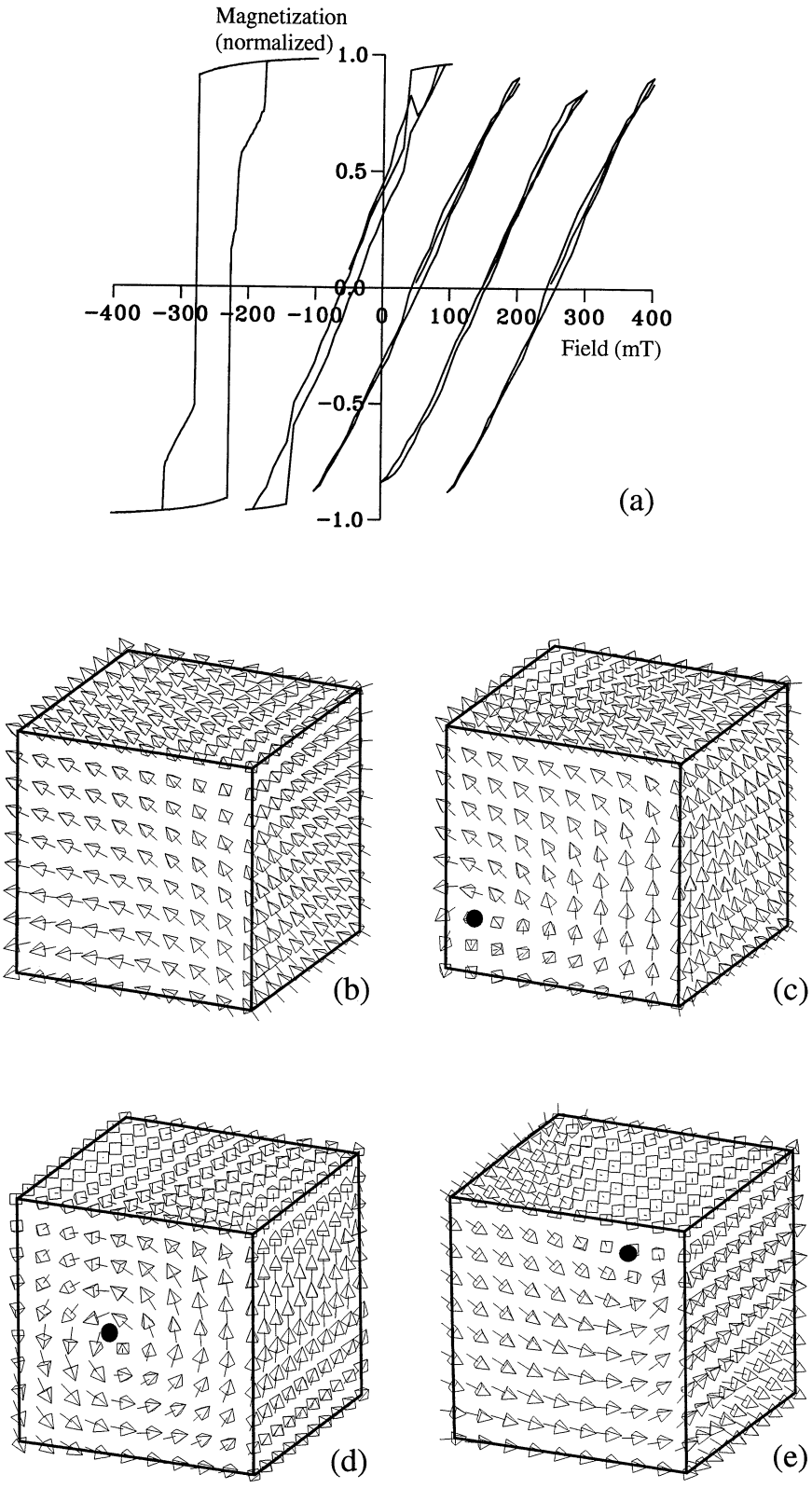

Figure 7. (a) The hysteresis loops for a cube of magnetite, with the field applied along the easy axis for a grain of size 0.1 μm, 0.2 μm, 0.5 μm, 0.7 μm, 1.0 μm (left to right). (b) The zero-field magnetic structure for 0.1-μm grain, showing a flower state aligned along an easy <111> axis. The process of vortex nucleation and propagation in the 0.2-μm grain during the descending branch of the hysteresis loop is shown at fields of (c) 80 mT (vortex nucleation), (d) -20 mT (vortex propagation), and (e) -90 mT (vortex denucleation). The solid circle indicates the vortex center.

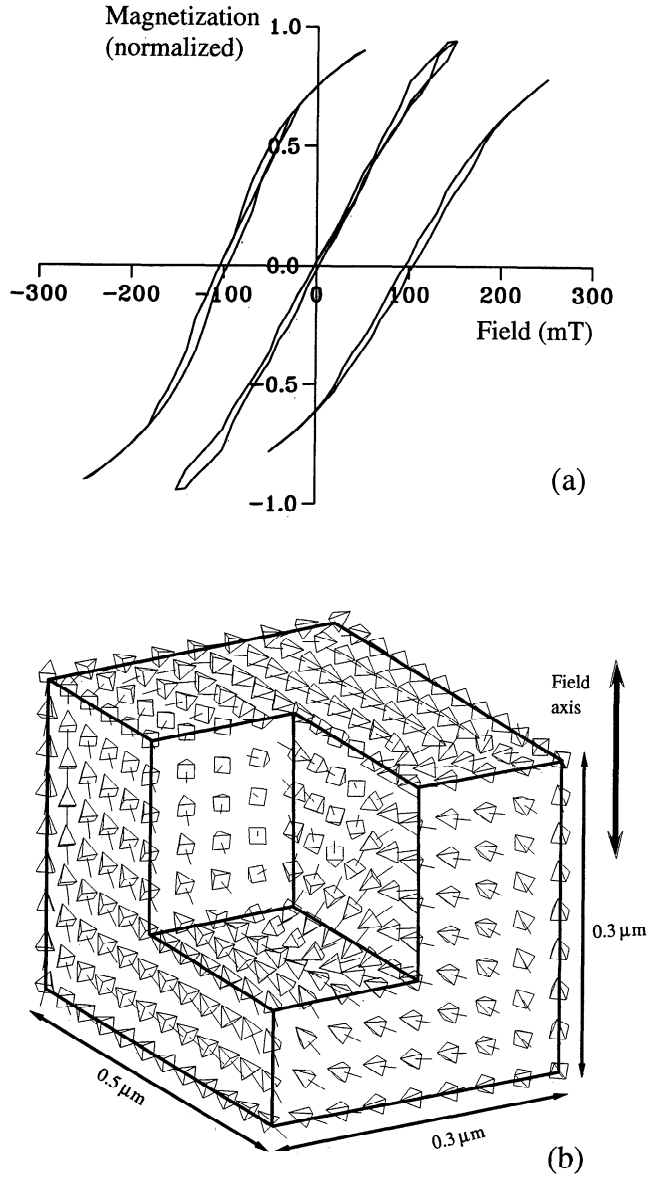

Figure 8. (a) The hysteresis loops for a $0.3 \times 0.3 \times 0.5$ μm elongated grain of magnetite, for the field directed along a short axis, the long axis, and a magnetocrystalline easy axis (left to right). (b) The zero-field stable magnetic structure (after hysteresis cycling) for the case where the field is applied along a short axis of the grain.

tex mode is still a stable zero-field state, it now requires the core and surface magnetizations to point in opposite directions, resulting in a structure similar to that obtained for the 0.2-μm grain at a later stage of the hysteresis cycle (Figure 3d). Comparison of the hysteresis loops for the 0.2-μm and 0.3-μm grains (Figure 3a and Figure 4a, respectively) shows that the effect of the increased internal demagnetizing field for the larger grain is to force the Barkhausen jumps to occur at an earlier point of the hysteresis cycle than for smaller grains where the relative effect of the exchange coupling is greater.

The vortexlike domain configuration is the dominant domain state at zero field for the grain size range from just above the critical single-domain grain size (0.05 μm) to $\sim$ 0.7 μm and thus covers the most significant region (i.e., highest remanence) of the pseudo-single-domain grain size range. A vortex structure is the equilibrium state even in elongated grains (see Figure 8b) and thus is likely to be a major contributor to the magnetic signal of rocks containing submicron grains of magnetite.

The switching of the magnetization in the 0.1-μm grain from one stable SD state to the antiparallel SD (i.e., flower) state occurs at a coercivity of 21 mT (hard direction) or 28 mT (easy direction), which is considerably smaller than the theoretically predicted value of 35 mT for coherent rotation of magnetization, opposed by magnetocrystalline anisotropy, in a cubic grain of magnetite of this size. The minimum energy transition is noncoherent (it is in fact a vortex mode), and so the coercivity is controlled by the intermediate domain states rather than by magnetocrystalline anisotropy.

This configurational anisotropy (i.e., anisotropy controlled by the domain configuration within the grain [see *Schabes and Bertram*, 1988a] is evident in elongated grains also. Although the grain shape is important in determining the exact nature of the domain structure, the structures do not differ significantly from those already described for cubic grains. Furthermore, the vortex propagation mechanism is seen to be equally favored in elongated and cubic grains, and the energy barrier between reverse domain states in this case (unlike coherent rotation) does not depend critically on grain shape. Similar magnetization reversal processes have been reported by *Schabes and Bertram* [1988a, b], although they were not investigated in terms of vortex nucleation and propagation.

Comparison With Experimental Results

The predicted values of saturation remanence (M_{rs}) and coercivity (H_c) can be compared with experimental hysteresis measurements on laboratory prepared samples of pure magnetite separated into narrow grain size ranges. Some care must be taken when comparing the theoretical and experimental results, since the experimental samples all contain randomly oriented assemblies of grains. In principle, the coercivity and remanence should be calculated for a number of discrete orientations of the grain and the results integrated over a sphere to produce an average coercivity and remanence for the assembly of grains. In practice, it is not feasible to calculate hysteresis loops at many different angles to the field because of the large amount of computer time required. However, results were calculated for the hard and easy directions in most cases, and these should provide an estimate of the maximum and minimum values of saturation remanence and coercivity. Thus for each grain size, two values of H_c (Figure 9a) or M_{rs} (Figure 9b) are plotted, and the difference between the two values reflects the effect of magnetocrystalline anisotropy on hysteresis parameters at each grain size. For the small grains of magnetite which contain perfectly uniform magnetization the effect of magne-

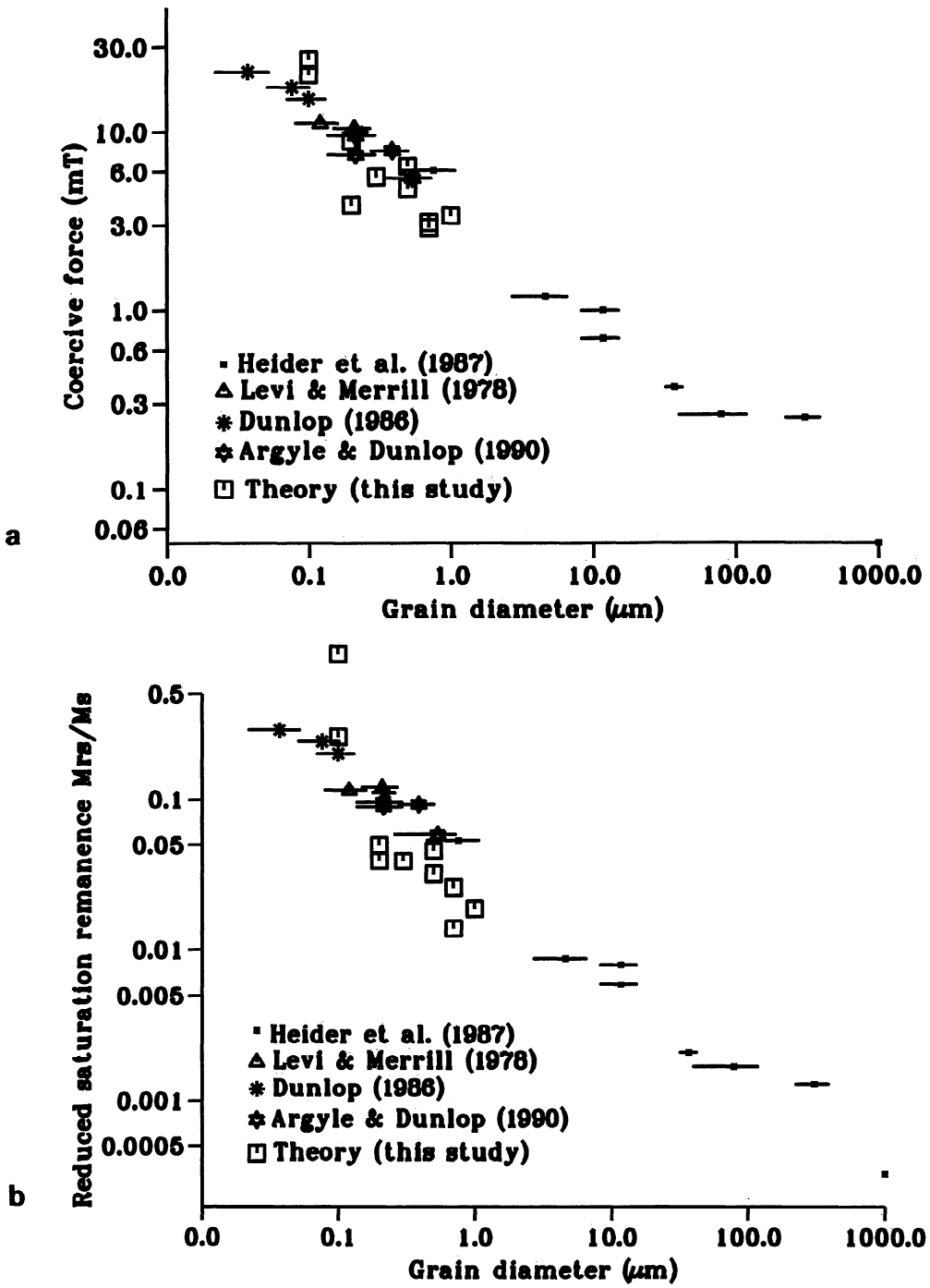

Figure 9. The theoretical predictions of (a) coercivity and (b) saturation remanence obtained from the hysteresis loops of Plates 2-8 compared with experimental data on laboratory-grown magnetites.

tocrystalline anisotropy is significant [*Stoner and Wohlfarth*, 1948]. However, for the grain sizes examined here, which contain nonuniform domain structures, the effect of anisotropy is seen to be quite small, with the exception of the M_{rs} values for the smallest grain size (0.1 μm) modeled.

There is reasonably good agreement between experimental and simulated hysteresis values, and thus we may have some confidence in the accuracy of the theoretically predicted domain structures and domain mechanisms. The predicted coercivity values (Figure 9a) are in good agreement with data for magnetite grains produced by hydrothermal recrystallization which do not contain many dislocations. This agreement of experimental and theoretical values suggests that in unstressed grains the barrier to reversal of the magnetization is not controlled by impurities or dislocations but purely by domain state and the configurational anisotropy.

The fact that the predicted values of saturation remanence (Figure 9b) are slightly lower than observed values may be due to the presence of SD grains in the

experimental PSD grain samples, which would tend to increase their measured values of M_{rs}, although this would also increase the value of H_c.

Pseudo-Single-Domain Grains and the Single-Domain-Multidomain Boundary

The PSD transition range between single-domain and multidomain grains has great significance for paleomagnetism. Samples containing well-dispersed single-domain grains are capable of holding a remanence whose behavior with temperature and over time is far better understood than that of multidomain grains. Stability of magnetic remanence in single-domain grains is thought to be determined by shape or crystalline anisotropy, whereas multidomain grains have more variable stability, determined by the pinning of domain walls by dislocations.

The switching behavior exhibited in the simulated hysteresis loops now provides a constraint on the analytical models of PSD grains. The magnetization reverses by discontinuous and continuous processes: a combination of rapid rotation of discrete regions of the grains (causing Barkhausen jumps) and gradual movements of domain walls and/or reversal of vortexlike regions. In the smallest of grains we modeled (0.1 μm), most of the grain volume switches via a single Barkhausen jump. As the grain size increases, the regions that undergo Barkhausen jumps decrease in size as a proportion of the total grain volume, while the number of these regions in the grain increases.

There are three main theories of PSD grain behavior: (1) SD-type inclusions within MD-type grains [*Verhoogen* 1959; *Banerjee*, 1977], (2) domain wall moments [*Dunlop*, 1977], and (3) failure of domain wall nucleation in MD grains [*Halgedahl and Fuller*, 1980].

The first of these theories cannot be accurately tested with micromagnetism given the present resolving power of the technique. However, grains above 0.05 μm in size are not truly single domain and yet cannot be said to contain SD inclusions surrounded by softer MD regions. Thus, although SD-like inclusions in larger grains (1 – 10 μm) cannot be ruled out, this mechanism cannot be regarded as a general model to explain the magnetic properties of PSD grains less than about 1 μm in size.

The second theory is based on one-dimensional models of domain structure, i.e., that the domain structure is lamellar and that grains just above the critical single-domain threshold have most of their volume occupied by a domain wall. This was further examined by one-dimensional micromagnetic models [*Enkin and Dunlop*, 1987], which determined the properties of PSD grains dominated by domain wall moments. In three-dimensional solutions, lamellar domain structures are not favored in the grain size ranges examined so far (up to 1.0 μm); instead, vortexlike structures are the equilibrium or lowest energy states.

The third theory assumes that there are no PSD grains as such but rather that samples are made up of a mixture of MD and SD grains, where grains in the SD state above the critical SD grain size have failed to nucleate domain walls. Experiments demonstrate that the fraction of PSD magnetite grains remaining magnetized after low-temperature demagnetization have alternating-field demagnetization spectra indicative of SD grains [*Dunlop and Argyle*, 1991], so that the grains demagnetized at low temperatures had remanences that were controlled by domain walls pinned at dislocations. These walls become unpinned as the wall widths increase in response to the magnetocrystalline anisotropy (K_1) vanishing at the isotropic point (130 K) [see *Dunlop*, 1990], effectively removing the MD component of the magnetization.

The magnetic structures described in this paper do not support the idea of grains of size 0.1 μm to 1.0 μm having their domain structure strongly controlled by crystalline anisotropy. It can be seen from Figures 9a and 9b that the coercivity and saturation remanence are relatively independent of whether the external field is applied parallel to the hard or easy directions. Furthermore, the zero-field structures are not significantly altered when the magnetocrystalline, exchange and saturation magnetization constants are changed to values appropriate to the isotropic point of magnetite (determined by extrapolation of measurements of exchange constant [*Heider and Williams*, 1988] and magnetocrystalline anisotropy constant [*Flecher and O'Reilly*, 1974] between room temperature and the Curie point), i.e., 0.0 Jm^{-3}, 1.47×10^{-11} Jm^{-1}, and 5.1×10^5 Am^{-1} respectively. However, the saturation remanences are somewhat lower than those found experimentally (see Figure 9b), indicating that a substantial fraction of grains may be in metastable SD states. If this is the case, it is not clear why low-temperature demagnetization should cause the nucleation of vortex states, unless the domain structures are influenced by factors such as magnetostrictive energies which have not been included in the present model.

Conclusions

Our simulations of hysteresis in submicron magnetite give values of H_c which are in good agreement with measurements on bulk samples, but values of saturation remanence are significantly lower than those observed. This indicates that the SD state is stable to larger sizes than predicted by our numerical models, but domain stability does not appear to be substantially influenced by magnetocrystalline anisotropy at room temperature or below.

The general features of experimentally observed hysteresis loops are reproduced by our simulations. Irreversible Barkhausen jumps occur in small PSD grains, and a combination of continuous and discontinuous changes occur in larger grains. The number of Barkhausen jumps increases and the size of the jumps decreases, as the grain size increases. Smooth movements of domain walls begin to appear in grains of $\sim$ 0.7 μm in size.

The dominant zero-field domain structure in both cubic and elongated grains is a vortex state. The relatively

close agreement of our theory with experiment indicates that such structures are probably the dominant states in small PSD magnetite grains. The magnetization reversal mechanism is by vortex nucleation and propagation, similar to that already predicted in zero-field states where reversals would occur with the help of thermal fluctuations [*Enkin and Williams*, 1994].

Acknowledgments. This research was supported by a British Government NERC grant GR3/7705 to W.W. and a NSERC Canada grant A7709 to D.J.D. We thank D. Blythe of the Ontario Centre for Large Scale Computation for his assistance in producing a video showing the magnetic structure changes in grains of various sizes during simulated hysteresis (available from the authors) and Song Xu for helpful comments on the manuscript.

References

Argyle, K. S., and D. J. Dunlop, Low-temperature and high temperature hysteresis of small multidomain magnetites (215-540 nm), *J. Geophys. Res., 95*, 7069–7082, 1990.

Banerjee, S. K., On the origin of stable remanence in pseudo-single-domain grains, *J. Geomagn. Geoelectr., 29*, 319–329, 1977.

Dunlop, D. J., The hunting of the "psark", *J. Geomagn. Geoelectr., 29*, 293–318, 1977.

Dunlop, D. J., Hysteresis properties of magnetite and their dependence on particle size: A test of pseudo-single-domain remanence models, *J. Geophys. Res., 91*, 9569–9584, 1986.

Dunlop, D. J., Developments in rock magnetism, *Rep. Prog. Phys., 53*, 707–792, 1990.

Dunlop, D. J., and K. S. Argyle, Separating multidomain and single-domain-like remanences in pseudo-single-domain magnetites (215-540 nm) by low-temperature demagnetization,*J. Geophys. Res., 96*, 2007–2017, 1991.

Enkin, R., J., and D. J. Dunlop, A micromagnetic study of pseudo-single-domain remanence in magnetite, *J. Geophys. Res.*, 92, 12,726–12,740, 1987.

Enkin, R. J., and W. Williams, Three-dimensional micromagnetic analysis of stability in fine magnetic grains, *J. Geophys. Res., 99*, 611-618, 1994.

Flecher E. J., and W. O'Reilly, Contribution of Fe^{2+} ions to the magnetocrystalline anisotropy constant K_1 of $Fe_{3-x}Ti_xO_4$ ($0 < x < 0.1$), *Phys. Rev. A, 7*, 171–178, 1974.

Halgedahl, S. and M. Fuller, Magnetic domain observations of nucleation processes in fine particles of intermediate titanomagnetite, *Nature, 288*, 70–72, 1980.

Heider, F., and W. Williams, Note on the temperature dependence of exchange constant in magnetite, *Geophys. Res. Lett., 15*, 184–187, 1988.

Heider, F., D. Dunlop, and N. Sugiura, Magnetic properties of hydrothermally recrystalized magnetite crystals, *Science, 236*, 1287–1290, 1987.

Landau, L. D., and E. M. Lifshitz, On the theory of the dispersion of magnetic permeability in ferromagnetic bodies, *Phys. Z. Sowjet. union, 8*, 53–169, 1935.

Levi, S., and R. T. Merrill, Properties of single-domain, pseudo-single-domain and multidomain magnetite, *J. Geophys. Res., 83*, 309–323, 1978.

Schabes, M. E., Micromagnetic theory of non-uniform magnetization processes in magnetic recording particles, *J. Magn. Magn. Mater., 95*, 249–288, 1991.

Schabes, M. E., and H. N. Bertram, Magnetization processes in ferromagnetic cubes, *J. Appl. Phys., 64*, 1347–1357, 1988a.

Schabes, M. E., and H. N. Bertram, Ferromagnetic switching in elongated γ-Fe_2O_3 particles, *J. Appl. Phys., 64*, 5832–5834, 1988b.

Stacey F. D., and S. K. Banerjee, *The Physical Principles of Rock Magnetism*, Elsevier, New York, 1974.

Stoner, E. C., and E. P. Wohlfarth, A mechanism of magnetic hysteresis in heterogeneous alloys, *Philos. Trans. R. Soc. London A, 240*, 599–642, 1948.

Verhoogen, J., The origin of thermoremanent magnetization, *J. Geophys. Res., 64*, 2441–2449, 1959.

Williams, W., and D. J. Dunlop, Three-dimensional micromagnetic modelling of ferromagnetic domain structure, *Nature, 337*, 634–637, 1989.

Williams, W., and D. J. Dunlop, Some effects of grain shape and varying external magnetic field on the magnetic structure of small grains of magnetite, *Phys. Earth Planet. Inter., 65*, 1–14, 1990.

D. J. Dunlop, University of Toronto, Department of Physics, Toronto, Ontario, Canada M5S 1A7.

W. Williams, University of Edinburgh, Department of Geology and Geophysics, West Mains Road, Edinburgh EH9 3JW, Scotland. (e-mail: Wyn.Williams@edinburgh.ac.uk)

(Received February 8, 1994; revised October 19, 1994; accepted November 2, 1994.)